ISSN 0029-3865

CNPq

CBPF - CENTRO BRASILEIRO DE PESQUISAS FÍSICAS

Notas de Física

CBPF-NF-054/93

Nucleation-Evaporation Model for Multifragment Emission

by

K.C. Chung

Rio de Janeiro
1993

ABSTRACT

Nuclear fragmentation processes are simulated in the nucleation–evaporation picture, with charge and energy conservations. The impact parameter and excitation energy per particle are parametrized as a linear function of the effective interaction radius R_{int}. The calculated IMF multiplicity and the charge distributions as well as the energy spectra are compared with recent 4π experimental results.

Key-words: Nuclear fragmentation; Nucleation; Evaporation.

PACS numbers: 25.70.Np; 64.60.Qb

1. INTRODUCTION

Recently, nucleation model was used by several authors to simulate the breakup of a hot nuclear system into many pieces [1,2,3]. In particular, it was shown that the fragment mass and charge distributions of nuclear fragmentation can be reasonably reproduced, if the "critical" value of the effective interaction radius R_{int} is adopted within the scheme of the nucleation model [3].

However, it should be noted that the energy spectra are left out in all the previous nucleation work. The main reason is that the nucleation model, just like the percolation models [4,5,6], treats the (dis)assembly of nucleons as a cold process, without any mention to excitation energy and, in consequence, it can not be expected to cover the two–dimensional phase diagram of the fragmenting nuclear system. Of course, a realistic description of nuclear fragmentation processes requires the introduction of a new ingredient, namely, the temperature of the system, which, for this purpose, is assumed in thermodynamical equilibrium for simplicity. This assumption is indeed consistent with recent experiments performed by Louvel *et al.* [7].

In the other hand, nucleation can produce quite exotic configurations, such as filamented or hole-endowed or very ramified structures. Once again, this is the same case than in percolation models. Naturally, all of these clusters can not be identified with final state nuclear fragments, but only with excited primordial ones. As a matter of fact, this idea is supported by position-sensitive hodoscope measurements [8]. So, it is mandatory to include evaporation or other secondary decays, if comparison with experimental data is to be done.

In this paper, we present a simple model which incorporates explicitly the evaporation process in the nucleation description of the nuclear fragmentation. Doing that, we expect to be able to describe more realistically some recent 4π experimental results, namely, the fragment kinetic energy spectra, the charge and IMF multiplicity distributions.

First of all, the temperature is introduced indirectly by a simple ansatz, relating the effective interaction radius R_{int} and the excitation energy per particle

ϵ^* which, with the help of the thermal droplet model [9], can be expressed as function of the temperature T. It should be noted that the present work takes into account the isospin degrees of freedom and, in every event, the computation obeys charge and energy conservations. Furthermore, a simple parametrization of the impact parameter as function of R_{int} is also included. We consider only the main evaporation channels, namely, the evaporation of neutron, proton and light composites like deuteron, triton, ^3He and alpha particles [10]. The relative probabilities are calculated by using the Weisskopf statistical theory of evaporation [11].

The scheme of this paper is the following: in section 2, we outline the main points of the nucleation-evaporation model and the Coulomb expansion following the breakup. In section 3, we discuss both the dependence of the effective interaction radius upon the impact parameter and the *ansatz*, relating R_{int} and the excitation energy ϵ^*. In section 4, for completeness, we address the evaporation rates. At last, results and discussion are given in section 5.

2. NUCLEATION AND COULOMB EXPANSION

The main idea of nucleation is that each constituent of the nuclear system can be involved by an effective interaction sphere of radius R_{int}, and that each nucleon will interact with another only when the interdistance is less or equal to $2R_{int}$. In this case, one nucleon is trapped by another and then the nucleons are said connected.

The multifragment formation is simulated by a conventional Monte Carlo method, where the position $\mathbf{r_i}$ of every nucleon of the nuclear compound system is randomly chosen inside a sphere of radius R, corresponding to the volume of the expanding system right before it breaks-up into many pieces. Nucleon interdistances less than the hard-core radius $R_c = 0.4fm$ are prohibited. Nuclear surface effects are taken into account, by randomly selecting the magnitude of each $\mathbf{r_i}$ according to a trapezoidal distribution for the nuclear density. Then, a simple algorithm is used to classify the clusters, which are defined in a standard way as a subset of connected nucleons such that there is a continuous path linking every nucleon of the cluster but there is no path connecting nucleons located in different clusters. As mentioned in the Introduction, this definition does not prevent the appearance of quite exotic clusters, or still worse, of completely pathological structures, with a disconnected topology like two interlaced rings.

The actual simulation of the breakup of a system formed by A_o nucleons, with Z_o protons and $N_o = A_o - Z_o$ neutrons, assumes the initial system, due to the compression heating, to expand from the initial radius R_o to the final value

R, such that $R = \alpha R_o$, where α is the expansion factor. It is very reasonable to consider α to lie between 1.44 and 2.00, which corresponds to a final density between 1/3 and 1/8 of the normal nuclear density $\rho_0 = 0.153 fm^{-3}$. This scenario seems to be most suitable to central nucleus-nucleus collisions at intermediate beam energies ($E/nucleon \gtrsim 30 MeV$). In fact, it is expected that, in this case, thermal pressure may arise and lead hot nuclear systems to expand until density fluctuations grow exponentially, provoking ultimately the total desintegration of the nuclear system.

With relation to the cluster charges, we assume in a very naïve manner the N_o/Z_o ratio to be almost invariant under the clusterization process. Especifically, for each cluster with A nucleons, we select randomly Z protons, such that the N/Z ratio be approximately equal to N_o/Z_o. For very light clusters, however, we impose $N/Z = 1$ for $A = 2$ and 4, and equal 2 for $A = 3$. For isolated nucleons, the charge is simply attributed by chance. However, a strict charge conservation for every partition $\{N_{Z,A}\}$ is assured, *i.e.*,

$$\sum_{Z,A} N_{Z,A} Z = Z_o. \tag{1}$$

Right after the break-up of the hot nuclear system, the Coulomb forces begin to dominate and lead the excited clusters to repeal each other.

During the Coulomb expansion the fragments may undergo one or more particle evaporation processes before the dynamical asymptotic state is attained. However, for simplicity, we assume that the Coulomb expansion timescale is much smaller than the evaporation timescale. This allows us to treat the latter processes only after the whole Coulomb expansion is completed.

We assume the following initial conditions for the Coulomb expansion: The position $\mathbf{r}_i$ of the cluster i is taken as the center-of-mass of all the nucleons belonging to the cluster. The momenta $\mathbf{p}_i$ are randomly chosen, according to a Maxwell-Boltzmann distribution, at the temperature of the partition. For the sake of simplicity, we have assumed afterwards that each cluster has a spherical shape with the center coinciding with the center of the cluster, and the radius given by the usual relationship $R = r_0 A^{1/3}$, with $r_0 = 1.16 fm$. Furthermore, the cluster masses are given by the semi-empirical nuclear mass formula, so that the binding energy effects are taken into account, at least roughly.

The equations of motion are integrated numerically and it proceeds until the kinetic energy of each fragment ceases to show significant changes. At this point, the excited fragments are allowed to evaporate particles (Section 4). The final momenta of all the fragments are Lorentz transformed by the velocity of the center-of-mass of the projectile and target nuclei.

After each sampling, the fragments are stored and the procedure is repeated untill the statistics is considered satisfactory.

III. IMPACT PARAMETER AND TEMPERATURE

One possible way to introduce the impact parameter b dependence in the nucleation simulation is allowing the effective interaction radius R_{int} to depend upon b. However, this dependence can not be deduced, but has to be assumed. In this work, we adopt the simplest one, namely, a linear parametrization:

$$R_{int}(b) = R_c + \xi(1 + \frac{b}{R_0}), \tag{2}$$

where R_c is the hard-core radius and ξ is found, averaging $R_{int}(b)$ over a number of randomly chosen values of b, such that the final result reproduces the "critical" effective interaction radius R_{int}^{cr}, with R_{int}^{cr} being obtained in cold and $b = 0$ calculations [3]. Eq.(2) is somewhat arbitrary, but it is restricted to reproduce qualitatively general features in the limiting cases, namely, for central collisions ($b \to 0$) where the compression-expansion effect is larger, the fragment multiplicity is also larger and this means that R_{int} has to be smaller than in the case of peripheral collisions ($b \to R_0$). In addition, as the peripheral collisions are more probable than central ones, the impact parameter values are chosen according to a triangular distribution.

In the other hand, to introduce temperature, we allow the excitation energy per particle ϵ^* to depend upon R_{int}. This relationship is very hard to work out from fundamental processes. However, a naïve parametrization can be guessed by using very general considerations. As a matter of fact, in the limit $R_{int} \to R_c$, all the constituents of the system are isolated and it is reasonable to associate this configuration to a parent one with highest excitation energy. In the opposite case, for $R_{int} \to R$, only one cluster is formed and this corresponds to a lowest excitation energy parent configuration. Between these two limits, once again, a linear parametrization is assumed for simplicity, *i.e.*,

$$\epsilon^* = \epsilon_0^*(R - R_{int})/(R - R_c), \tag{3}$$

where ϵ_0^* is the value of ϵ^* for $R_{int} = R_c$, a situation which corresponds, as mentioned above, to completely dissolved nucleons. In this case, it is natural to assume ϵ_0^* to have the same value of the nuclear binding energy per particle ($8MeV$). Then, the thermal droplet model will provide the desired relationship between R_{int} and T.

In this point, the energy conservation requires every partition $\{N_{Z,A}\}$ to satisfy:

$$E_{total} = E_0^{ground} + \epsilon^* A_0 = \sum_{Z,A} N_{Z,A} E_{Z,A}, \tag{4}$$

where E_0^{ground} stands for the groundstate energy of the fragmenting system and $E_{Z,A}$, the total energy of the fragment (Z, A). However, we follow Ref.[9] which projects out the Coulomb contribution due to a homogeneously charged sphere of charge $Z_0 e$ and volume $V = \frac{4}{3}\pi R^3$, *i.e.*,

$$E_{total} - \frac{3}{5}\frac{Z_0^2 e^2}{R} = \sum_{Z,A} N_{Z,A} E'_{Z,A}. \tag{5}$$

In this case, the internal fragment energy is given by:

$$E'_{Z,A} = (W_0 + \frac{T^2}{\epsilon_0})A + (\beta - T\frac{d\beta}{dT})A^{2/3} + \gamma\frac{(A-2Z)^2}{A} + \frac{3}{5}\frac{Z^2 e^2}{R_{Z,A}}(1 - \frac{1}{\alpha}) + \frac{3}{2}T \tag{6}$$

where $\beta = \beta_0 \{(T_c^2 - T^2)/(T_c^2 + T^2)\}^{5/4}$.

The coefficients $W_0 = -16MeV$, $\beta_0 = 18MeV$ and $\gamma = 25MeV$ are the usual droplet model parameters; $\epsilon_0 = 16MeV$, the level-density parameter at normal nuclear matter density; $T_c = 16MeV$, the critical temperature and $R_{Z,A}$, the fragment radius. The last term in the righthand side of Eq.(6) accounts for the kinetic energy of the fragment. See Ref.[9] for more details.

IV. EVAPORATION RATES

The de-excitation of the hot clusters can be treated by using the Weisskopf's statistical theory of the evaporation [11], if the clusters, right after the break-up, are assumed in thermodynamical equilibrium. In the following, we outline the procedure used in Ref.[10]. First, as usual, the probability per time unit for emission from a nucleus A of a particle j with kinetic energy between E and $E + dE$ can be calculated by

$$P_j(E)dE = \gamma_j \sigma E exp(S_f - S_i)\, dE \tag{7}$$

where: $\gamma_j = g_j m_j/\pi^2\hbar^3$, and $\sigma = \sigma_0\,(1 - V_j/E)\,\theta(E - V_j)$, with σ_0 denoting the cross section for the inverse reaction; θ the step function; $S_{f(i)}$, the entropy of the final (initial) nucleus; V_j the Coulomb barrier corrected for the nuclear temperature; and g_j and m_j the number of spin states and the mass of the particle j, respectively.

However, since the time evolution of the evaporation probabilities is not relevant, the relative probabilities have been used, *i.e.*,

$$\frac{P_j}{P_1} = \frac{\gamma_j}{\gamma_1}\frac{E_j^*}{E_1^*}\frac{a_1}{a_j} exp\left[2\left(\sqrt{a_j E_j^*} - \sqrt{a_1 E_1^*}\right)\right] \tag{8}$$

where the a_j's are defined by the statistical model level density formula, *i.e.*, $\rho_j \propto exp[2(a_j E_j^*)^{1/2}]$ and E_j^* is the excitation energy of the nucleus after evaporating a particle j. The coeficientes a_j's have been parametrized according to the procedure proposed by LeCouter [12].

After each evaporation process, it is assumed that the residual nucleus reaches the equilibrium immediately. The evaporation procedure is repeated, until the excitation energy of the residual nucleus decreases below the threshold for particle evaporation.

V. RESULTS AND DISCUSSION

In what follows, we consider the nuclear system formed by the projectile and target nuclei. Two specific reactions are focused here, namely, $^{36}Ar + {}^{197}Au$ ($110\,MeV/nucleon$) and $^{129}Xe + {}^{197}Au$ ($50\,MeV/nucleon$ of bombarding energy). These reactions have been analysed by the MSU 4π Miniball detector, and we have in mind three types of outcome: charge distribution, IMF ($3 \leq Z \leq 20$) multiplicity and kinetic energy spectrum for fixed angle and charge.

In our simulation (4000 runs in the case of $Ar + Au$ and 6000 runs in $Xe + Au$ system), we have neglected the incomplete geometrical coverage and finite detection thresholds of the experimental apparatus. These effects are expected not to change our results qualitatively.

First of all, we assume the expansion factor $\alpha = 1.71$, or what is the same, $\rho = \rho_0/5$. This value seems to be consistent with several statistical and hydrodynamical model calculations. In fact, different values of α, within the range of

interest here, have been ckecked and the results show that the qualitative features are essentially the same.

The "critical" effective interaction radius, in this case, is calculated to be $R_{int}^{cr} = 1.3fm$ for both systems [3]. Central collisions events were selected by the same criterion adopted in Fox *et al.* [13], namely $b/b_{max} \leq 0.2$ $(Ar + Au)$, and in Bowman *et al.* [14], namely $b/b_{max} \leq 0.3$ $(Xe + Au)$, with b_{max} taken as the sum of the target and projectile nucleus radii.

In Fig.1, we display the calculated charge distributions (squares) and the experimental data (triangles) for central events in the case of $Ar + Au$ (top panel) and $Xe + Au$ (bottom panel) reactions with data taken from Phair *et al.* [15]. For $Ar + Au$ system, the agreement is very nice, which is observed in almost the whole range of Z, but for $Xe + Au$, the model calculation overpredicts the $Z = 1$ fragment population. However, the qualitative behaviour of the data is reproduced.

In Fig.2, the calculated energy spectra for boron $(Ar + Au)$ and carbon isotopes $(Xe + Au)$ are displayed for $\theta_{lab} = 19.5^o$, 27^o and 35.5^o (squares) and are compared with the experimental data from Fox *et al.* [13] and Bowman *et al.* [14] (balls), respectively, for central events. The Maxwellian behaviour of the experimental distributions seems to be very well reproduced in the case of $Ar+Au$ reaction. For $Xe+Au$, however, the present simulation underestimates the energy spectrum for 19.5^o and overestimates the number of very high energetic carbon isotopes for less forward angles.

The calculated IMF multiplicity distribution, for the $Ar + Au$ reaction, is plotted in Fig.3 (upper left panel) for three different gates N_c. It should be noted that the gate N_c, defined here as the total charged fragment multiplicity excluding the number of isolated protons, is slightly different from the experimental definition, which is given in Phair *et al.* [15] as the number of detectors in which at least one charged particle is recorded.

Keeping this difference in mind, we assume to be allowed to display, in the lower left panel of Fig.3, the experimental data of de Souza *et al.* [16] for the same ranges of N_c. It can be seen that the qualitative features of the data are described by the present calculation. As a matter of fact, the calculated curves display the same behaviour than the experimental ones and the average number of IMFs also increases with N_c. However, the peak of the calculated curve corresponding to the central events $(N_c \geq 32)$ is dislocated toward larger multiplicities. It should be noted that the calculated mean IMF multiplicity for central collisions is 5.5, while the measured value is 4.0.

Similarly, for the $Xe + Au$ reaction, the upper right and the lower right panels of Fig.3 show the calculated IMF multiplicities for the gates indicated

in the diagram and the data from Bowman *et al.* [17], respectively. The curve corresponding to central collisions have similar behaviour than the experimental data. In this case, the mean value is 6.2, which is very close to the measured result of 6.5. The curves for lower multiplicity windows, however, fail in reproducing the data.

It is not clear for us yet why the calculated results reproduce so nicely the $Ar + Au$ data, but not the $Xe + Au$ ones. It should be mentioned that this difficulty, in the specific case of charge distributions, has been already detected in percolation [15] and in nucleation [3] calculations. The inclusion of evaporation in the nucleation computation has narrowed the discrepancies only slightly. Some suggestions have been proposed, involving dynamical effects during the early nonequilibrium stages of the reaction or incorporating the dynamics of collective expansion or rotation [15]. This important question has to be investigated in future works, including other suggestions, like symmetry and relativistic effects.

Now, it is worthwhile to investigate how the average IMF multiplicity $\langle M \rangle_{IMF}$ in the nucleation-evaporation model changes with respect to the breakup density. In Fig.4, we display $\langle M \rangle_{IMF}$ as function of the density ρ. It is seen that $\langle M \rangle_{IMF}$ increases with the breakup density, at least in the density ranges considered here, and for $3 \leq \rho_o/\rho \leq 8$, it ranges from 4 to 7 ($Ar + Au$) and from 4 to 9 ($Xe + Au$). This dependence is a direct consequence of the introduction of the temperature and impact parameter degrees of freedom. Indeed, it is interesting to remind that in the cold and $b = 0$ nucleation calculations, $\langle M \rangle_{IMF}$ is almost insensitive to changes in density [3].

Finally, it is interesting to note that the average breakup temperature and the power-law exponent of charge distributions, in this model calculation, are 3.5 MeV and 2.6 for $Ar + Au$ reaction, and 4.3 MeV and 2.5 for $Xe + Au$ reaction, respectively. These figures are within the range of values assumed or obtained by several other models.

In summary, we have tryed to show that the main outcomes of exclusive experiments involving $Ar + Au$ and $Xe + Au$ reactions at 110 and $50 MeV/nucleon$, respectively, can be satisfactorily described by the nucleation-evaporation model. In particular, the charge distribution, the IMF multiplicity distribution and the kinetic energy spectra have been simultaneously calculated by a model which is based on very simple assumptions, namely, thermodynamical equilibrium, probabilistic considerations, linear parametrization both for impact parameter and excitation energy. It has been shown also that the whole computation was done, by using only one free parameter – the expansion factor α. As this nucleation-evaporation model succeeds in reproducing several aspects of the experiments, one suggestion seems to be in order, that this fact may be an indication that the multifragment emission from hot nuclear system is basically a simple dice game.

FIGURE CAPTIONS

Fig.1: Charge distributions for central collision events. The curves are normalized in $Z = 1$.

Fig.2: Kinetic energy spectra for boron (upper panels) and carbon fragments (lower panels) in central collision events at $\theta_{lab} = 19.5^o, 27^o$ and 35.5^o. The calculated curves are normalized to the maximum of the experimental spectra.

Fig.3: Calculated (upper panels) and measured (lower panels) IMF multiplicities for different gates N_c of the total charged fragment multiplicity. The distributions are normalized to unit area.

Fig.4: Average IMF multiplicity as function of ρ_o/ρ.

Figure 1:

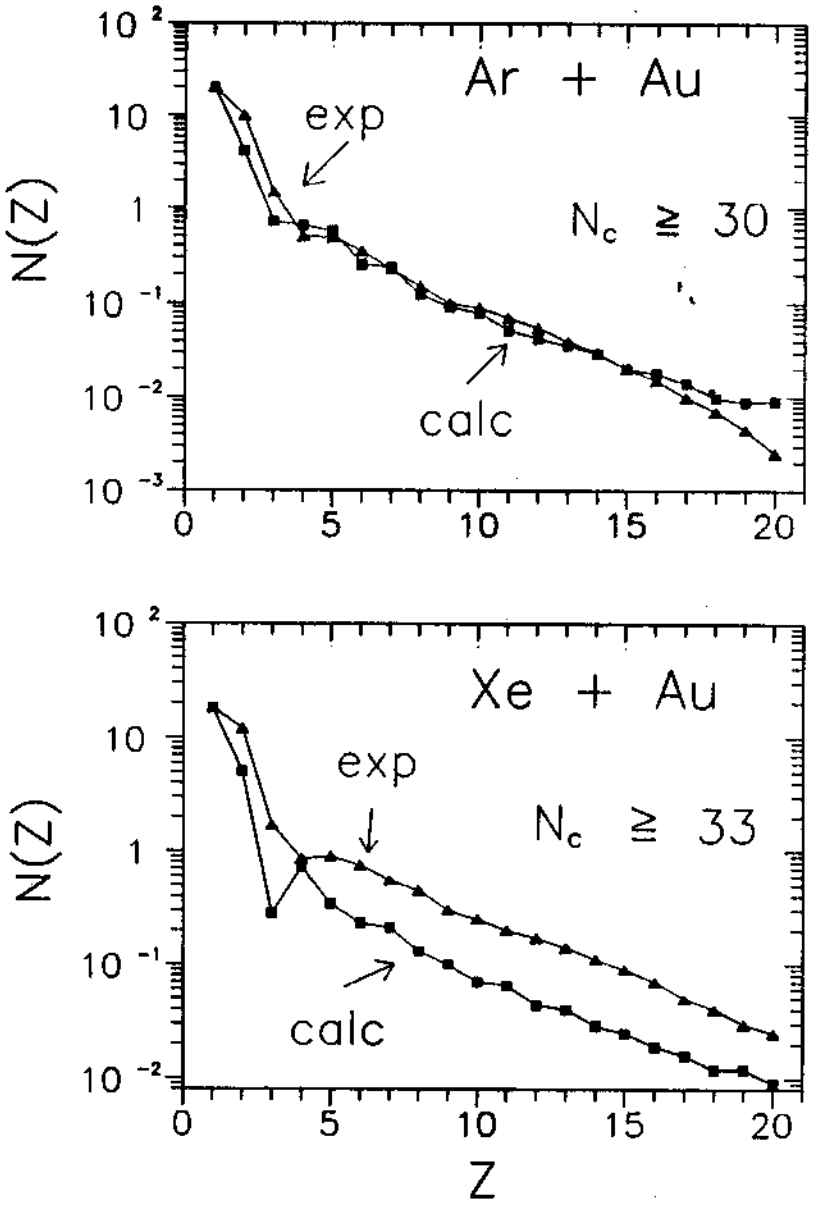
Ar + Au
exp
calc
$N_c \geq 30$
Xe + Au
exp
calc
$N_c \geq 33$
N(Z)
Z
10^2
10
1
10^{-1}
10^{-2}
10^{-3}
0
5
10
15
20

NUCLEATION-EVAPORATION MODEL ... by K.C. Chung

Figure 2:

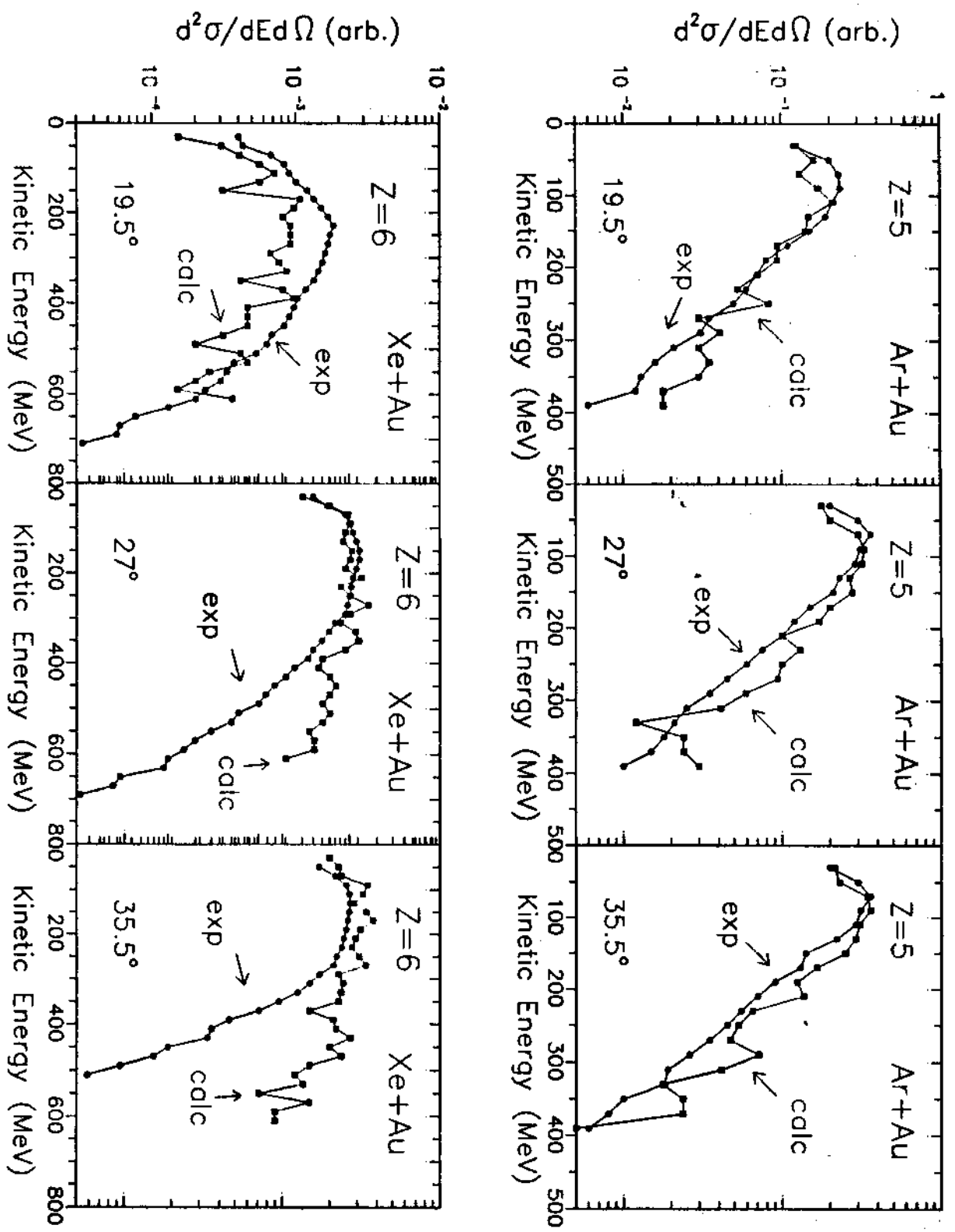

Figure 3:

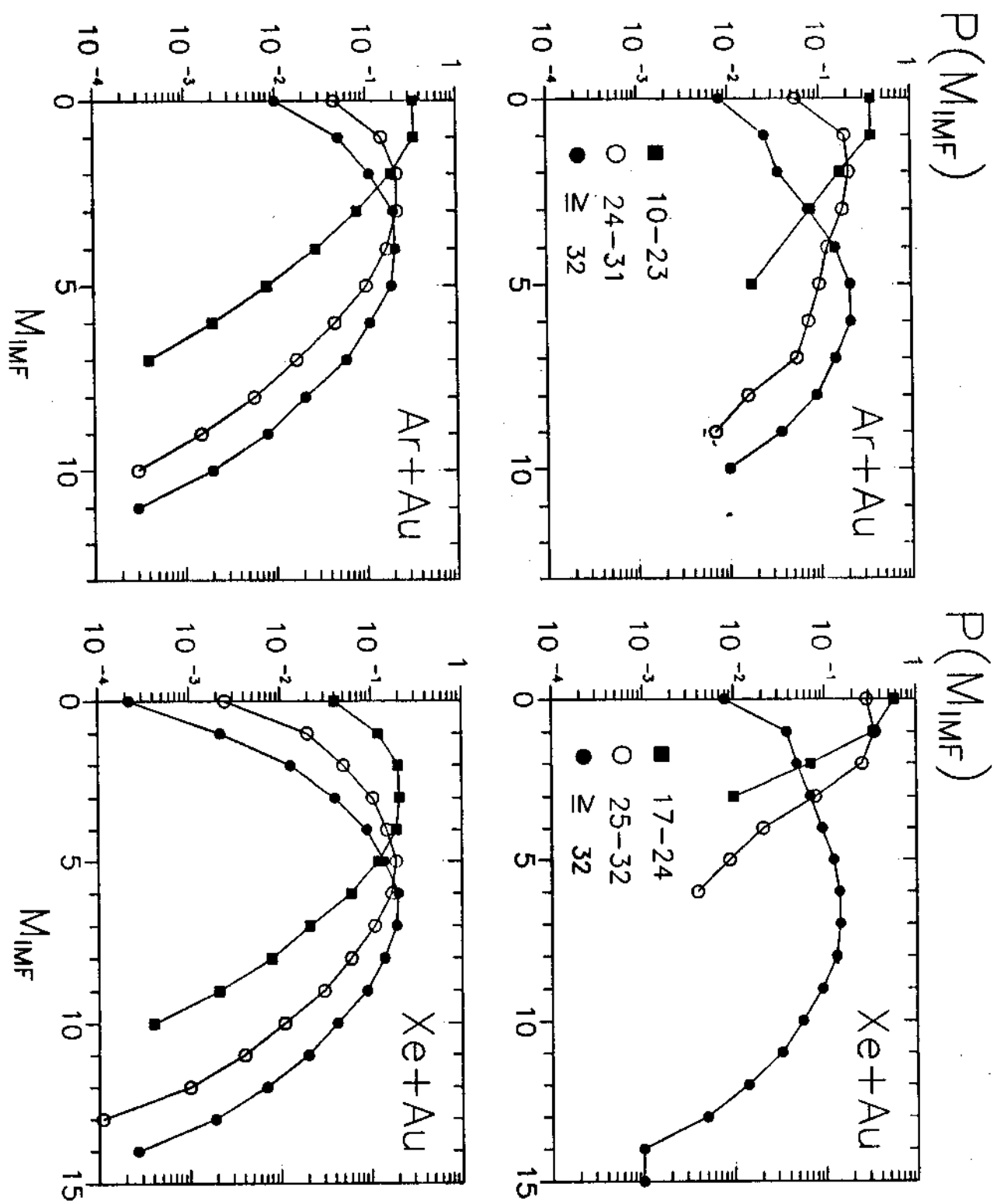

NUCLEATION-EVAPORATION MODEL ... by K.C. Chung

Figure 4:

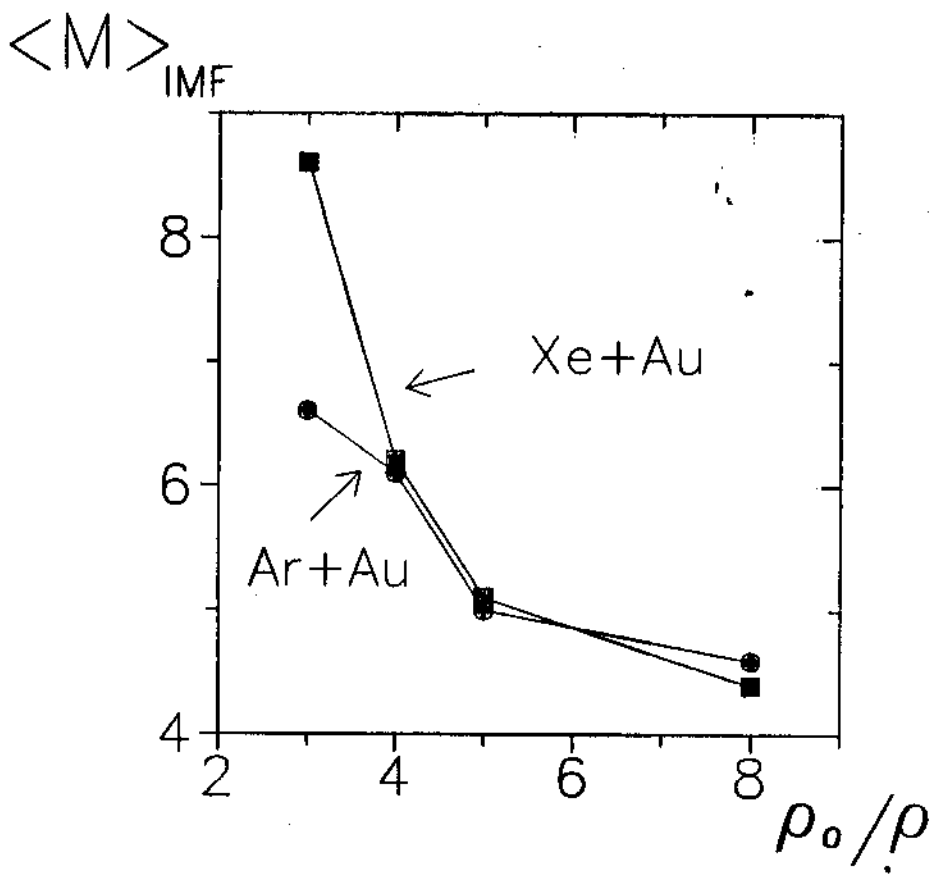

REFERENCES

1. C.O. Dorso and R. Donangelo, Phys. Lett. **B244**, 165 (1990).
2. C. Ngô, H. Ngô, S. Leray, and M.E. Spina, Nucl. Phys. **A499**, 148 (1989).
3. K.C.Chung, to be published in J. of Phys. G.
4. X. Campi and J. Desbois, *Proceedings of the 23rd International Winter Meeting on Nuclear Physics (Bormio)*, 1985.
5. W. Bauer, D.R. Dean, U. Mosel, and U. Post, Phys. Lett. **150B**, 53 (1985).
6. N.C. Chao, and K.C. Chung, J. of Phys. **G 17**, 1851 (1991).
7. M. Louvel, T. Hamdani, G. Bizard, R. Bougault, R. Brou, H. Doubre, D. Durand, Y.El Masri, H. Fugiwara, A. Genoux-Lubain, K. Hagel, A. Hajfani, F. Hanappe, S.C. Jeong, G.M. Jin, S. Sato, J.L. Laville, C. Le Brun, J.F. Lecolley, S. Lee, T. Matsuse, T. Motobayashi, J.P. Patry, A. Péghaire, J. Péter, N. Prot, R. Regimbart, F. Saint-Laurent, J.C. Steckmeyer and B. Tamain, Nucl. Phys. **A559**, 137 (1993).
8. T.K. Nayak, T. Murakami, W.G. Lynch, K. Swartz, D.J. Fields, C.K. Gelbke, Y.D. Kim, J. Pochodzalla, M.B. Tsang, H.M. Xu, F. Zhu, and K. Kwiatkowski, Phys. Rev. **C 45**, 132 (1992).
9. J.P. Bondorf, R. Donangelo, I.N. Mishustin, C.J. Pethick, and H. Schulz, Nucl. Phys. **A444**, 460 (1985).
10. A.J. Santiago, and K.C. Chung, J. of Phys. **G 16**, 1483 (1990).
11. V. Weisskopf, Phys. Rev. **52**, 295 (1937).
12. K.J. LeCouter, Proc. Phys. Soc. **A63**, 259 (1950).
13. D. Fox, R.T. de Souza, L. Phair, D.R. Bowman, N. Carlin, C.K. Gelbke, W.G. Gong, Y.D. Kim, M.A. Lisa, W.G. Lynch, G.F. Peaslee, M.B. Tsang and F. Zhu, Phys. Rev. **C 47**, R421 (1993).
14. D.R. Bowman, C.M. Mader, G.F. Peaslee, W. Bauer, N. Carlin, R. T. de Souza, C.K. Gelbke, W.G. Gong, Y.D. Kim, M.A. Lisa, W.G. Lynch, L. Phair, M.B. Tsang, C. Williams, N. Colonna, K. Hanold, M.A. McMahan, G.J. Wozniak, L.G. Moretto and W.A. Friedman, Phys. Rev. **C 46**, 1834 (1992).
15. L. Phair, W. Bauer, D.R. Bowman, N. Carlin, R.T. de Souza, C.K. Gelbke, W.G. Gong, Y.D. Kim, M.A. Lisa, W.G. Lynch, G.F. Peaslee, M.B. Tsang, C. Williams, F. Zhu, N. Colonna, K. Hanold, M.A. McMahan, G.J. Wozniak and L.G. Moretto: Phys. Lett. **B285**, 10 (1992).

16. R.T. de Souza, L. Phair, D.R. Bowman, N. Carlin, C.K. Gelbke, W.G. Gong, Y.D. Kim, M.A. Lisa, W.G. Lynch, G.F. Peaslee, M.B. Tsang, H.M. Xu, F. Zhu and W.A. Friedman: Phys. Lett. **B268**, 6 (1991).

17. D.R. Bowman, G.F. Peaslee, R.T. de Souza, N. Carlin, C.K. Gelbke, W.G. Gong, Y.D. Kim, M.A. Lisa, W.G. Lynch, L. Phair, M.B. Tsang, C. Williams, N. Colonna, K. Hanold, M.A. McMahan, G.J. Wozniak, L.G. Moretto and W.A. Friedman, Phys. Rev. Lett. **67**, 1527 (1991).